A Dynamic Physical Model of Cell Migration, Differentiation and Apoptosis in *Caenorhabditis elegans*

Antje Beyer[1], Ralf Eberhard[2,3], Nir Piterman[4], Michael O. Hengartner[2], Alex Hajnal[2], and Jasmin Fisher[5]*

[1]Department of Genetics, University of Cambridge, Cambridge, UK, [2]Institute of Molecular Life Sciences, University of Zurich, Zurich, Switzerland, [3]PhD Program in Molecular Life Sciences, Life Science Zurich Graduate School and MD/PhD Program, University of Zurich, Zurich, Switzerland, [4]Department of Computer Science, University of Leicester, Leicester, UK, [5]Microsoft Research, Cambridge, UK,

*corresponding author

Abstract The germ line of the nematode *C. elegans* provides a paradigm to study essential developmental concepts like stem cell differentiation and apoptosis. Here, we have created a computational model encompassing these developmental landmarks and the resulting movement of germ cells along the gonadal tube. We have used a technique based on Molecular Dynamics (MD) to model the physical movement of cells solely based on the force that arises from dividing cells. This novel way of using MD to drive the model enables calibration of simulation and experimental time. Based on this calibration, the analysis of our model shows that it is in accordance with experimental observations. In addition, the model provides insights into kinetics of molecular pathways within individual cells as well as into physical aspects like the cell density along the germ line and in local neighbourhoods of individual germ cells. In the future, the presented model can be used to test hypotheses about diverse aspects of development like stem cell division or programmed cell death. An iterative process of evolving this model and experimental testing in the model system *C. elegans* will provide new insights into key developmental aspects.

1 Introduction

Since the early 1970s (1), the nematode *C. elegans* has been a widely studied model in biomedical research (reviewed in e.g. (2-5)). Through the worm's transparent body it is possible to trace any cell by light microscopy or to study gene expression and cellular development *in situ* (6). The fixed number of cells of the somatic cell lineages have been meticulously described (cf. (7)) and are invaluable for the genetic analysis of regulatory pathways in development (cf. (8)) or in neurobiology. The germ line of *C. elegans* allows for the observation of several essential developmental processes like stem cell proliferation, gametogenesis, and programmed cell death, also termed apoptosis. Importantly, these biological processes are spatially well resolved in this system, where germ cells mature in sequential steps along a tube-shaped gonad. It has therefore been extensively used in basic research (reviewed in (9-12)). Other than the highly predictable development of somatic tissues, cellular events in the germ line seem to be very stochastic; consequently the underlying general mechanisms are little understood for some of these processes. This is particularly true for physiological germ cell apoptosis. Programmed cell death is a crucial developmental process that is found in many different species; aberrations in this program have important implications in complex diseases like human cancers (13) or neurodegenerative disorders (14). It is therefore key to gain fundamental understanding of its mechanisms. In this work, we propose a computational model of the germ line that is mainly based on physical properties and which aims to provide more insights into the previously mentioned developmental processes. With our model, we are able to test hypotheses about the causes and mechanisms of programmed cell death, among other developmental processes, and to highlight promising theories to be validated experimentally.

The *C. elegans* Germ line
The reproductive system of *C. elegans* has a symmetric structure with two U-shaped gonads extending from a single vulva, one anteriorly and one posteriorly. Our model considers the development from stem cells to mature oocytes within one gonad (see Fig. 1). Although the nuclei and their cytoplasm within the germ line are not completely encapsulated cells and thus are part of a syncytium, they are usually referred to as germ "cells". As the differential interference contrast (DIC) picture and the electron microscopy imaging in Fig. 1 indicate, the cytoplasmic membranes are not fully delimiting, leaving a connection of all cells to a common shared cytoplasm in the centre of the gonad tube, called rachis.
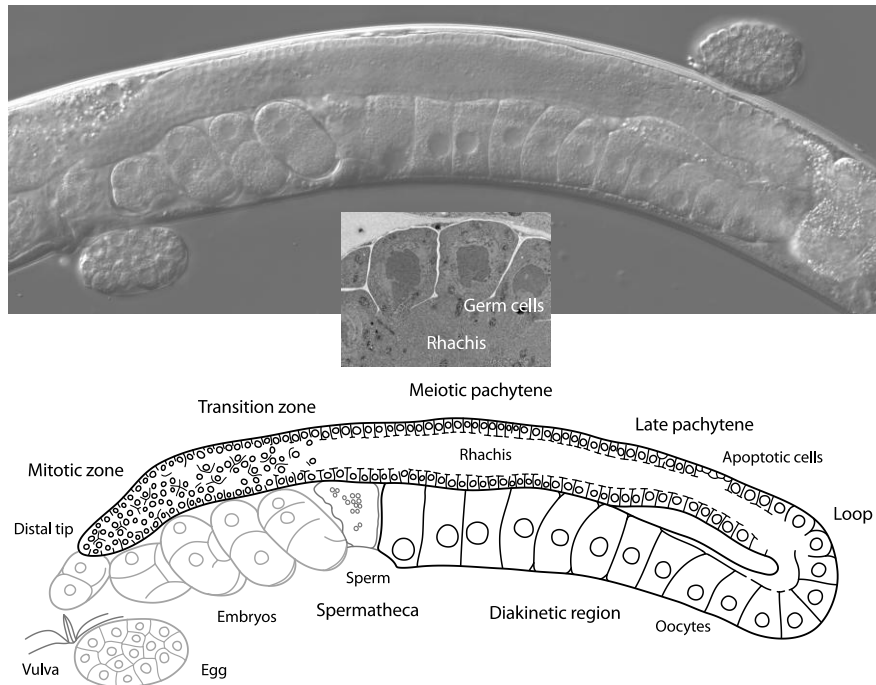
Fig. 1 The germ line of *Caenorhabditis elegans* by DIC (top), as a schematic (bottom), and in a cross section (transmission electron microscopy). The head of the worm is to the right, the posterior gonad to the left of the picture. Differential interference contrast (DIC) microscopy allows to observe live animals in any focal plane; here, an adult hermaphrodite is virtually dissected along a plane through the centre of the gonad tube. The germ cells in the meiotic pachytene region form a monolayer around a concentric inner tube, seen as a nuclei-free area in the longitudinal and cross sections (rachis). The limits of the transition zone and of the late pachytene stage within the meitoc pachytene region are not strictly defined by DIC. The oocytes in the loop have exited pachytene and begin the diakinetic stage of meiosis.

The mature hermaphroditic germ line can be divided into functionally different zones with specific developmental properties (15-18). At the distal most end of the gonadal tube the mitotic zone is located ("distal" here meaning farthest from the uterus), containing dividing stem cells and representing a stem cell niche. The potential of the mitotoic cell pool to divide is maintained by molecular signals – directly via activation of proliferation or, more likely, indirectly via inhibition of differentiation. Delta ligand from extrinsic sources (the distal tip cell) activates the Notch pathway, promoting a high Notch within the germ cells of this region. In the transition zone, where no external Delta ligand is presented, the Notch level gradually decays. When the germ cells are left without Notch, they complete the mitotic cell cycle, enter meiosis and start their differentiation into oocytes (16). A small transition zone in which mitotic and first meiotic cells are interspersed links to a seemingly well orchestrated meiotic pachytene region, where chromosomes

undergo homologous recombination. At some point within the meiotic zone, the germ cells start growing at a low rate so that they have visibly increased their size by the time they reach the bend of the gonad and exit the pachytene stage of meiosis. In this loop region, the rachis is thinned to an eccentric tube, but still connecting the growing oocytes before they become proper cells with a fully closed membrane. Distal to the loop with the young oocytes, programmed cell death can be observed as part of normal oogenesis (19). Physiological apoptosis, the fate of about half of all germ cells, is considered to be restricted to this area of the gonad (11). Ras/MAPK activity is required for pachytene exit (20) and oocyte maturation; its absence also disables apoptosis (19). For our model, we premise that germ cells start accumulating Ras activity towards the end of the meiotic pachytene region, induced by an external Ras signal. If the Ras level surpasses a certain threshold in a germ cell, it starts to grow to become a fully grown oocyte filling the complete diameter of the tube when it reaches the proximal end of the gonad. We also assume here that the Ras level is decisive for germ cell death: it renders a cell capable for or insensitive to physiological apoptosis.
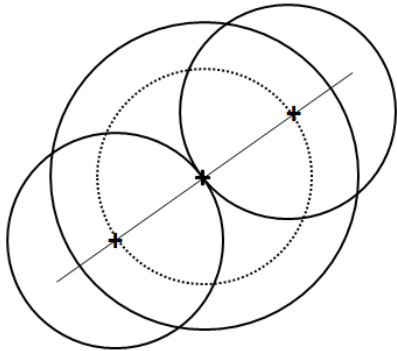
Molecular Dynamics Model

Fig. 2 Schematic representation of a dividing cell. The big circle represents the parent cell, the two diametrically positioned circles are the daughter cells, the centres of the three cells are represented by the + signs. The straight line signifies the division axis and the dotted circle is the imaginary circle with one basic radius around the centre of the parent cell on which the centres of the daughter cells are placed

Dividing cells in the mitotic zone apply pressure on the surrounding cells as the two daughter cells need more space than the parent cell (cf. Fig. 2). This leads to physical movement of the cells away from the pressure centre. We have constructed our model using an algorithm based on Molecular Dynamics (MD) modelling framework (21) to capture this movement according to the physical properties of each individual cell. This makes the movement of cells in our model very realistic so that we get a "virtual germ line". Apart from realistic movement, the MD framework allows for good visualisation and tracing of parameters for single or multiple cells. Originating from theoretical physics and chemistry to investigate

the behaviour and properties of various particles like planets or molecules, physical algorithms similar to MD have also been used in a few biological settings (22-27). In contrast to our specific modelling system, these MD models were applied to simulate the collective behaviour of tissues and aggregations of cells moving along a chemical or nutritional gradient. In these cases the physical movement through MD is just a side effect of the main movement along the gradient, while in our case the MD-movement is the main component of movement. In fact, it is the only driving source of movement; without the forces derived within the MD approach, the cells in our model would not move at all.

In addition to movement, we have built our MD-model to include developmental processes such as cell growth and division, as well as apoptosis, to make it sufficiently realistic. These processes depend on signals received by the cells according to their location in the tube. We show that our model reproduces cellular behaviour observed in experimental settings (15; 28; 29) very closely. This suggests that our model is a useful tool to gain novel insights into the core developmental processes observed in the *C. elegans* germ line.

2 Model

The main part of our model is the movement algorithm from Molecular Dynamics. We have used the *Velocity Verlet* algorithm (30), which is based on the following basic formula of Newtonian motion:

$$F = ma \qquad (1)$$

A Taylor series development of Formula (1) and some further transformations imply the following steps of the algorithm for each cell. We will elaborate them a little more in the subsequent two paragraphs.

Step 1: $\vec{v}(t + \frac{1}{2}\Delta t) = \vec{v}(t) + \frac{1}{2}\vec{a}(t)\Delta t$

Step 2: $\vec{x}(t + \Delta t) = \vec{x}(t) + \vec{v}(t + \frac{1}{2}\Delta t)\Delta t$

Step 3: Derive $\vec{a}(t + \Delta t)$ from the interaction potential using $\vec{x}(t + \Delta t)$.

Step 4: $\vec{v}(t + \Delta t) = \vec{v}(t + \frac{1}{2}\Delta t) + \frac{1}{2}\vec{a}(t + \Delta t)\Delta t$

Here, t represents the time and Δt signifies the time step of the execution which is usually very small. The variable $\vec{x}(t)$ represents the location at the current time, $\vec{v}(t)$ stands for the velocity at the current time and $\vec{a}(t)$ for the acceleration at the current time. In our model, we replace acceleration with the force and the mass based on Formula (1), i.e. $a = F/m$. For now, we simplify this further by assuming the mass to be one, which leads to $a = F$.

The first step of the algorithm computes the velocity at the intermediate time $t + 1/2\Delta t$, which is used in the next step to evaluate the location of the cell at the next time, $t + \Delta t$. Using this new location of the cell, the force working on it at time $t + \Delta t$ is derived from the so-called interaction potential in the third step. The interaction potential is a function describing how a particle, here a cell, interacts with its environment. In our case, the potential acts in such a way that the cell is pushed away from cells that overlap it and there is no force working on the cell if other cells do not overlap it. The force on the cell is stronger the more overlap there is. If more than one cell overlaps the cell, the forces are accumulated. In the last step of the algorithm, this new force is used to calculate the velocity at the next time $t + \Delta t$. This algorithm is computed for each cell and each time step Δt of the execution for a certain number of time steps.
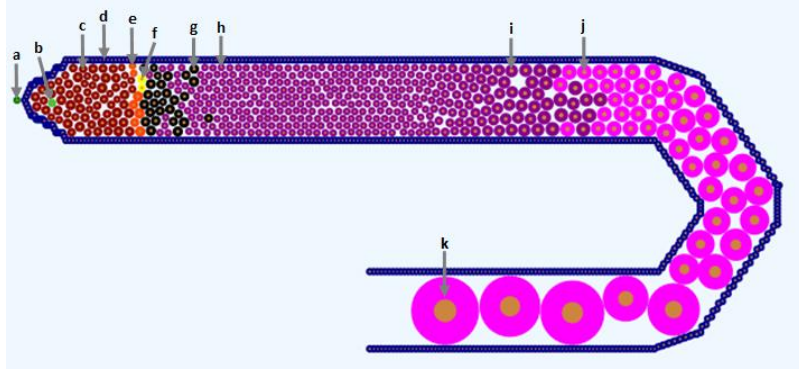

Fig. 3 Snapshot of an execution of the germ line model; a: Distal Tip Cell (dark green), b: marked cell (light green), c: mitotic cell with highest Notch level (dark red), d: cells defining the border of the tube (blue), e: mitotic cell with Notch level between highest and 0.5 times the highest level (orange), f: mitotic cell with Notch level between 0.5 times the highest level and 0 (yellow), g: mitotic cell with Notch level equal to 0 (black), h: meiotic cell (purple), i: meiotic cell that has grown to about twice its original size (purple), j: oocyte with Ras level above threshold (pink), k: fully grown oocyte (pink)

Since the algorithm works on a per cell basis, we have constructed the cells in our model as objects. To unite the functional style of the algorithm and the object oriented style of the cells, we have used the F# programming language (31), which incorporates both of these environments in a natural way. Additionally, the language also provides us with a very straightforward visual frontend. For simplification, our current model is a two-dimensional representation of the germ line as shown in Fig. 3. A movie of an execution of the model can be viewed at (32). The different colours are used to represent different states or component levels of the cells. To define the general structure of the germ line in our model we estimated germ cell numbers along the gonadal tube from microscopic pictures of the germ line. This provided us with estimates of cells across the tube diameter (cells per column in our model) and per developmental zone along the tube. The sizes of the

different zones of the germ line were translated into the range of pathway activation in our model.

2.1 Internal Properties of Cells

As previously mentioned, the cells in our model are represented as objects. All cells are described by the same object class; they all have the same general internal properties. The different values of these properties describe the cells' current status within the model. Differences in cell behaviour between cells arise from differences in the specific momentary environment and slight randomisations of certain internal properties. In this section, we will describe the most important of these internal properties and how their values are derived.

2.1.1 Location

Every cell has a specific 2-dimensional location assigned to it. The location is updated at each time step of the execution depending on the Velocity Verlet algorithm. The location is in continuous space as opposed to models which work with a grid of possible locations.

2.1.2 Velocity and Force

As previously mentioned, the Velocity Verlet algorithm computes the new cell locations based on the velocity and force that are acting on the cell. For this purpose, we have equipped each cell with 2-dimensional velocity and force vectors which are changed by the algorithm. The values of these two properties define the degree of change in the location through the Velocity Verlet algorithm.

2.1.3 Cell State

Another important property of the cells in our model is the state of a cell. We have defined the states "Mitotic" (c, e, f and g in Fig. 3) and "Meiotic" (h, i, j and k in Fig. 3) which depend on the location and the cell cycle state of the cells. We also mark dead and fertilised cells in this way to make them countable and to be able to remove them from the model. Furthermore, we defined a state "Stopped" (a and d in Fig. 3) that marks all boundary cells of the tube not to move and to form the walls of the germ line. This definition of the germ line walls does not exactly conform to nature, but it is a simplification for computation purposes that is sufficiently realistic.

2.1.4 Ras and Notch Level

The cells also contain variables defining their Ras and Notch levels. These are changed according to the environment at the cell's location along the tube as this informs about the presence of external ligand molecules for the two signalling pathways. Along the x-axis of the coordinate system of our model, the Delta ligand is active in the region from 3.8 (which is the beginning of the tube) to 22. From coordinate 22, the Delta ligand is turned off; this is where the transition zone starts. The external Ras is present from 75 up to the beginning of the bend at 117 when it is turned off. When Delta ligand is present, the Notch level within the cells will jump to its highest value (c in Fig. 3). The level decays linearly over time in the absence of ligand (from c to e to f to g, representing no Notch, in Fig. 3). The Ras level is accumulated linearly over time as long as the ligand is present.

2.1.5 Size and Growth

The cells are also assigned a size that is updated at each step of the execution. For simplicity, we consider our cells to be round. Hence, the size of a cell is its radius. The size of a cell changes as it progresses along the gonadal tube depending on the cell's status and location. All cells have the same basic size to which they go back after a division. The change of size is defined by growth functions common to all cells. An exception to this is the function defining the growth rate of mitotic cells that is randomised for each cell. This assures that cells which are born at the same time do not necessarily divide synchronously, but at slightly different times. This results in a more realistic timing of the cell divisions.

2.1.6 Analysis Parameters

The previously mentioned cell properties are all included to achieve a behaviour and movement of the cells that is as realistic as possible. We have also included a few parameters for purely analytical purposes.

GFP
All cells contain a variable GFP – named after the visual marker Green Fluorescent Protein in biological experiments – that can be turned on to visually follow this cell and its offspring in the simulation (b in Fig. 3). In addition, the data for these cells, i.e. the values of the previously mentioned parameters and the analytical parameters described below, can be read out to be analysed. If desired, this could be adjusted to track only one cell.

Density Factor
The cells also have a density factor associated with them. This density factor f of cell c is computed at each time step using the following equation:

$$\sum_{c_i \in N(c)} \frac{r_i}{6(d(c_i,c)-r_i)}$$

where $N(c)$ is the set of all cells touching cell c, r_i is the radius of cell c_i and $d(c_i,c)$ is the distance between the cells c_i and c. This factor is set to zero if no cell is touching c and to one if the neighbouring cells are ideally packed, i.e. c is surrounded by six cells of the same radius as c. The density is above one if other cells are overlapping c. This density factor could later be used to test hypotheses about the apoptotic mechanism.

Movement and Division Rates

To compare the movement rate of the cells with experimental findings, we have also introduced a list to represent this rate. A function writes each time step to this list in which the cell has moved at least one diameter along the x-axis compared to the location at the previously stored time step. Similarly to the movement rate, we have also defined a list representing the division rate. This list is appended by the current time step when the cell divides so that each cell carries a history of all previous divisions for its ancestors. This list is passed to both daughter cells upon a division.

2.2 Other Properties of the Model

The cells in our model are not standalone objects, but they interact with each other and their environment, i.e. the gonadal tube. The interplay between the internal configuration of the cells and their surroundings results in the behaviour that can be observed in the model. For the specification of these interactions, we have defined some general properties of the model which are described in this section.

2.2.1 Cell Growth and Division

Before they divide to form two daughter cells, cells marked as mitotic grow to a size of $\sqrt{2}$ times their basic radius, which corresponds to twice their area. The two daughter cells both have the same basic radius and are placed so that the distance of their centres is two basic radii (cf. Fig. 2). In the *C. elegans* germ cells the orientation of the division axis appears to be random. In our model, the daughter cells are placed symmetrically with regards to a random central division axis in their parental cell (straight line in Fig. 2). Their centres will thus be positioned diametrically on an imaginary circle around the centre of the parent cell with the basic radius (dotted circle in Fig. 2). The daughter cells inherit the Notch level and GFP status from their parent. At the same time the division rate list in the daughter cells is updated and a cell is added to a counter of the total number of cells.

2.2.2 Growth of Early Meiotic Cells and Oocytes

Meiotic cells stay at the basic radius until they reach a certain point in the tube from which they start growing slowly, i.e. their radius is increased, until they have reached about double their area right before the loop. When the Ras level within these cells has reached a certain threshold, they exit the pachytene stage of meiosis and proceed into diakinesis to become mature oocytes (j and k in Fig. 3). Initially, the radii of the oocytes grow about ten times faster than the ones of late pachytene cells and, as they reach the end of the loop, this growth rate is increased by another 10-fold. The oocytes stop growing when their diameter is the width of the tube (k in Fig. 3). All cell growth in our model is defined by an increase in radius and happens at linear rates.

2.2.3 Death

In vivo, programmed cell death is normally confined to the late meiotic pachytene region before the loop where some cells become apoptotic. Accordingly, we defined a death zone in our model. In the worm, the death zone seems to be dependent on the location of the oocytes. Hence, we have defined a death zone of fixed size which ends at the x-axis location of the eighth oocyte and begins at a fixed distance distal to it. At the moment, random cells within this death zone will be eliminated as soon as the amount of cells surpasses a certain number. As a constraint to random cell death, we defined an artificial Ras threshold, above which cells become insensitive to apoptosis; only cells below this level are selectable for cell death. This is a somewhat naïve approach to the induction of apoptosis; the present model is just preliminary in this respect. Once a cell has died, the time step number of its death is recorded for analysis purposes and the cell disappears from the model.

2.2.4 Fertilisation

For simplicity, we currently define a cell as being fertilised when it reaches the end of the tube. As with the dead cells, the time step numbers when fertilisations happen are recorded and the cells are removed from the model.

3 Results

3.1 Calibration

Table 1 Table showing different properties extracted from experiments and literature (Expected) and the according values derived from the present model (Model) with the translation of these values into real time in the fourth column

Rate	Expected	Model	
Movement rate	1 row/90 min	1 row/5250 steps	1h = 3500 steps
Time btw. divisions	20 h	40k to 90k steps	19.19 h
Death rate	2 cells/h	1.57 cells/3500 steps	2 cells/h
Fertilisation rate	2 cells/h	4.27 cells/3500 steps	4 cells/h

To calibrate the model, we extracted parameter values (shown in the first column of Table 1) from the literature and from our own videos of the germ line to compare with our model. Our observations have shown that, on average, it takes the cells 90 minutes to advance along the x-axis by the distance of their own diameter. Literature (28; 29) suggests that one mitotic cell cycle in the germ line is 16 to 24 hours. This calculates to an average time of 20 hours between divisions. For the death rate, our observations suggest that on average two cells die per hour per gonad arm, a value observed independently by many groups since the first characterisation of physiological germ cell apoptosis in *C. elegans* (19). The literature and our own observations further suggest that the average egg laying rate is about four eggs per hour per animal (15). We have to be careful to translate this for our model since we only consider one gonad, whereas the egg laying rate accounts collectively for both the anterior and posterior gonad. Consequently, we consider a fertilisation rate of 2 oocytes per hour per gonad arm as an approximation of the average over time.

As we will delineate in the following sections, our model produces values which are in correspondence with these expected experimental values.

3.1.1 Movement Rate

For the calculation of the movement rate, each cell is equipped with a list containing every time step at which the cell has moved a distance forward equal to its current diameter. To evaluate the time that each of these steps has taken, we calculated the difference between every two succeeding time steps. Fig. 4 shows a histogram of these differences for all of the cells within the model. The distribution looks basically like a Gaussian. The average movement rate in our model is 5250 steps for one diameter. Since we have observed the movement rate to be one

diameter per 90 minutes *in vivo*, we can derive here that 90 minutes is equivalent to approximately 5250 steps in our model. As a consequence, we can assume that one hour in real time is approximately 3500 steps in our model.
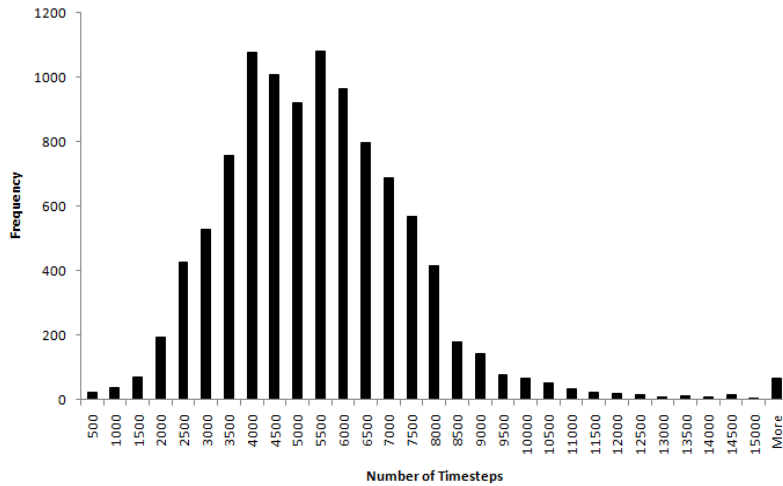

Fig. 4 Histogram showing a distribution of the number of time steps needed for the advancement of each cell by one diameter.
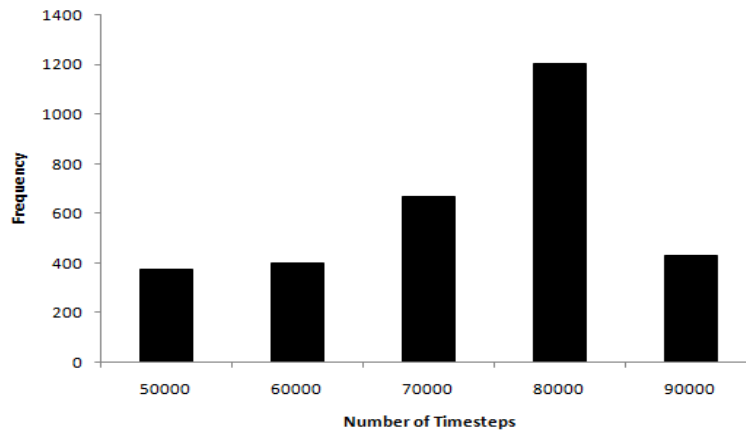
3.1.2 Time between Divisions

Fig. 5 Histogram showing the distribution of time steps between divisions for all cells

Each cell carries a list containing all time steps in which a division has occurred for this cell. By subtracting succeeding values, we have calculated the number of time steps between two divisions. Fig. 5 shows a histogram of these numbers for

all of the cells in the model. The values for the time between divisions range from 40,000 to 90,000 time steps. Using our estimation for real time from above, this is a range of 11 to 26 hours. The average of all times between divisions for all cells in our model is 67,158 time steps which evaluates to about 19 hours.
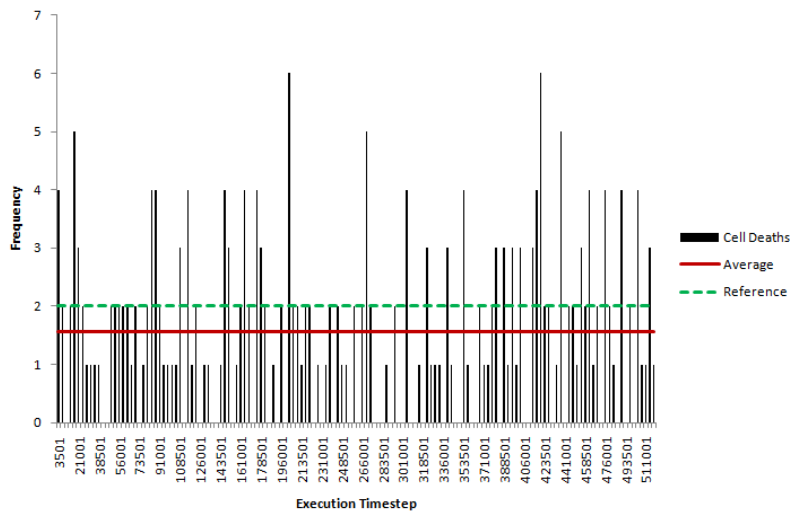
3.1.3 Death Rate

Fig. 6 Histogram of the number of cell deaths over bins of 3500 execution time steps. The continuous horizontal line indicates the average number of cell deaths per 3500 time steps, the dashed line shows the experimental reference

For each dead cell, we have recorded the time step number at which it died. To get an estimate of the death rate, we looked at bins of 3500 time steps, which is approximately one hour in real time (cf. Section 3.1.1). Fig. 6 shows a histogram of the number of cell deaths occurring in these bins during an execution. Averaged over all bins, this computes to 1.57 deaths per bin or, in real time, 1.57 deaths per hour (continuous horizontal line). The figure shows that our reference indicated by the dashed horizontal line is only slightly higher than the average resulting in the model.
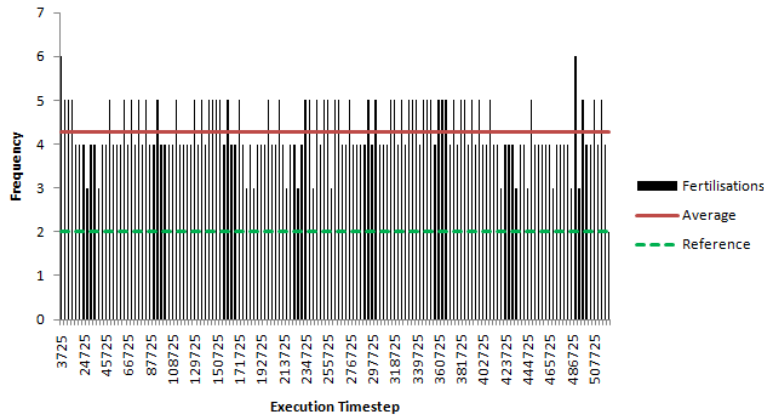
3.1.4 Fertilisation Rate

Fig. 7 Histogram of the number of fertilised cells over bins of 3500 execution time steps. The continuous horizontal line indicates the average number of fertilised cells per 3500 time steps, the dashed line shows the literature reference

We have also recorded the time step at which fertilisation occurred for each fertilised cell. In a similar fashion to the death rate, we have sectioned this data in bins of 3500 time steps to get an estimate of the fertilisation rate. Fig. 7 shows a histogram of the number of fertilisations per 3500 time steps. The figure also shows the average number of fertilisations per bin (or hour) which is 4.27 cells (continuous horizontal line). The literature reference, indicated by the dashed horizontal line in the figure, is lower than our model average.

3.1.5 Summary

Table 1 summarises the findings of our model calibration. Relative to the movement rate observed in our model, the time between divisions and the death rate in our model are very much in accordance with the values observed *in vivo*. Solely the fertilisation rate differs between our model and the experimental observations. These parameters are the major developmental components in our model. As a consequence, we can consider this model as, for our purposes, a very good approximation to the real organ since it reproduces the major developmental features very accurately.

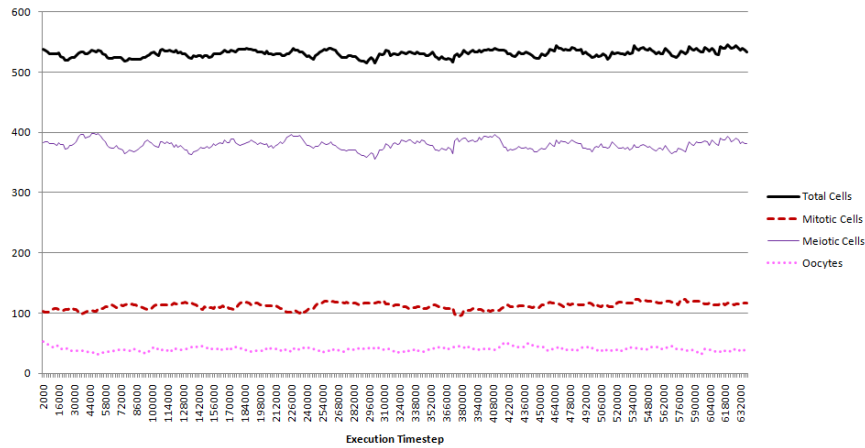## *3.2 Further Results*

3.2.1 Cell Numbers

Fig. 8 Graph showing the development of cell numbers over execution time; the thick continuous line represents the total number of cells, the thin continuous line stands for the number of meiotic cells, the dashed line is for the mitotic cells and the dotted line for the oocytes

Fig. 8 shows the development of cell numbers in the different developmental stages and of the total number of cells over execution time. One can see that our model is in a steady state in terms of cell numbers and that none of these values significantly fluctuates. This is in accordance with *in vivo* observations of the germ line of an adult wild-type animal (15; 28).

3.2.2 Density

Fig. 9 shows the average density in bins of about 1.5 basic cell radii from the distal end of the germ line up to the beginning of the loop. The average is taken of the density factors of all cells whose centre is within the respective bin. As defined earlier, a density factor of 1 represents an ideal packaging around an individual cell, while a factor of 0 indicates a cell that does not have neighbours that touch it. A value above 1 hence indicates overcrowding through overlap of neighbouring cells. Fig. 9 shows that the average density factor is relatively low. The figure also shows that the size changes of germ cells are especially important in terms of the density factor. In the region between 33 and 75, where there should be only few dividing cells – apart from a few outliers – and where the cells do not grow, the density is lowest and it does not fluctuate as much as in the other regions. The

16

changes in density by growth are especially apparent in the region from 75 up to the end of the plot. Apart from a dip between 105 and 109, the density constantly increases, which is also true for the size of the cells in this region. The dip in this increase could be due to space that is freed up by dead cells since this is the region of the tube where the death zone is located.
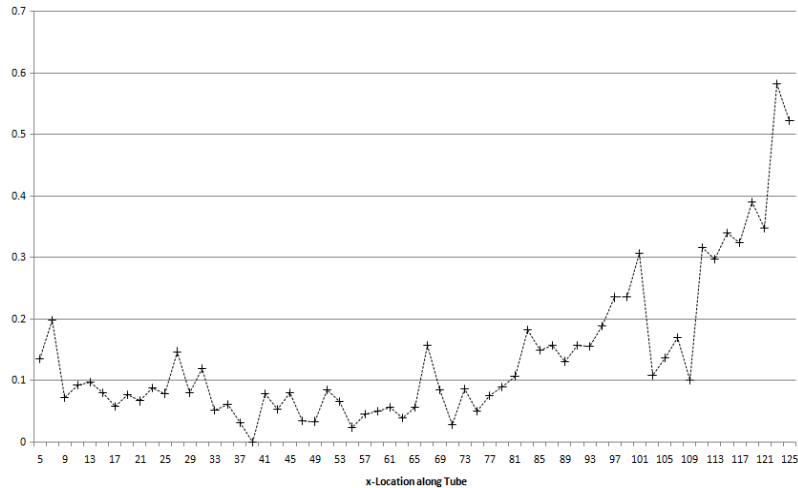

Fig. 9 Graph showing the average density along the germ line from the distal end up to the bend in bins of approximately 1.5 basic cell radii at execution step 734000

3.2.3 Following Marked Cells

As mentioned in the Model section, we are able to label cells in our model and follow them on their course through the germ line. Here, we have followed one cell and its 12 offspring to get more information about what happens to individual cells in our model.
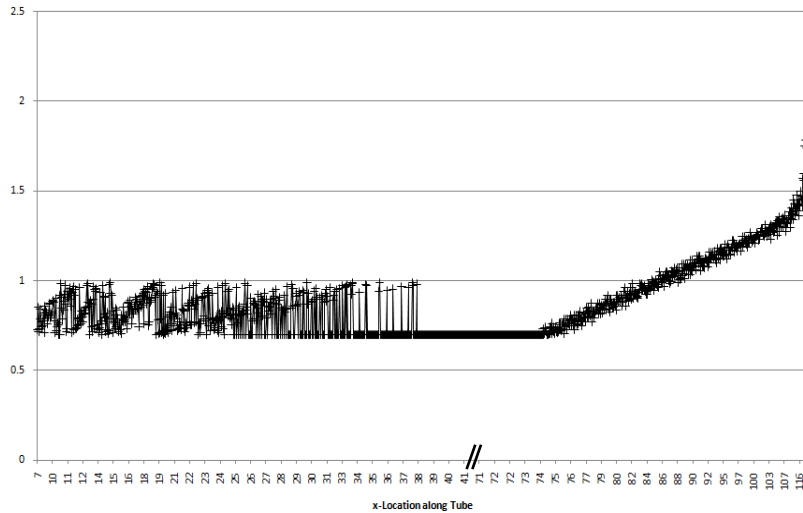
Fig. 10 Graph showing the sizes of the marked cells according to their location in the germ line from the distal end up to the bend during the whole execution

Fig. 10 depicts the development of size of these individually marked cells from the distal end up to the beginning of the loop. For illustration, we have excluded values ranging between 42 and 70 on the x-axis since the values remain constant. The figure shows that the size of cells in the mitotic zone and the transition zone ranges between 0.7 and a value just below 1. This is due to the fact that the basic cell size is 0.7 and dividing cells grow from this size up to $\sqrt{2} \cdot 0.7$ which is just below 1. From about 30 up to 37 there does not seem to be a smooth change of size but rather an oscillation between maximal and basic size. This indicates that cells of big size are pushed from the mitotic zone into this area of the germ line to divide there. They do not grow anymore since they enter meiosis after the division. This area represents the transition zone. The figure also shows that between about 37 and 75 there is no growth before a constant linear growth of the cells sets in. This growth changes to a much steeper one at the end which corresponds to the region of the tube where the first cells reach Ras levels above the threshold causing them to grow faster. This figure also underlines our assumptions in the previous paragraph that growth and division of cells are very important in the development of the density factor.
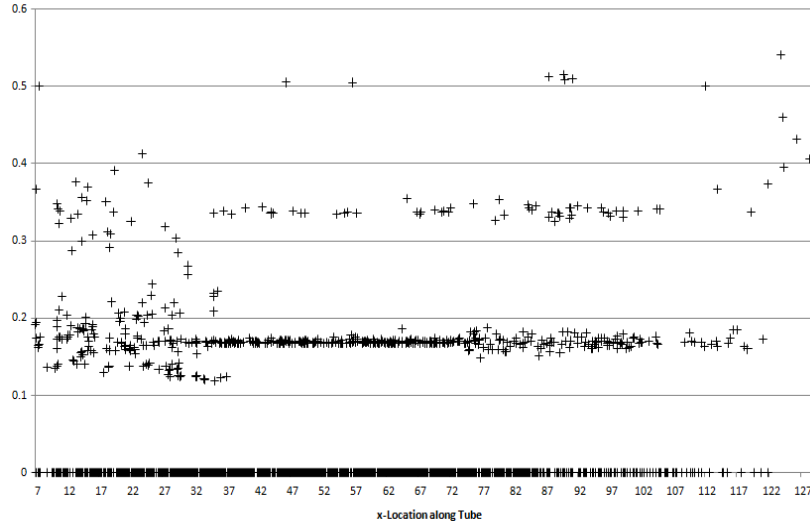
18

Fig. 11 Graph showing the density factors of the marked cells according to their location in the germ line from the distal end up to the bend during the whole execution

Fig. 11 shows the development of the density factor for the marked cells over the distance from the distal end of the gonad to the beginning of the loop. As in the averaged case, the density factor is generally fairly low. Since each mark in the graph stands for the density factor of one single cell, it is expected that the factor scatters more widely here. While some cells have a density factor of 0, others have one of more than 0.5. While in Fig 9 the average density is never above 0.2 up to about 95 on the x-axis, individual cells in Fig. 11 show several values above 0.2 and even some that are above 0.5 in the same region. Similar to Fig. 9, Fig. 11 also shows that in the region without cell growth and with only some division, i.e. between about 35 and 75 (cf. Fig. 10), the density stays relatively constant and there are more cells with very low density factors. In fact, Fig. 11 shows that from about 80, where growth is continuously strong, less and less of the marked cells retain a density factor of 0.
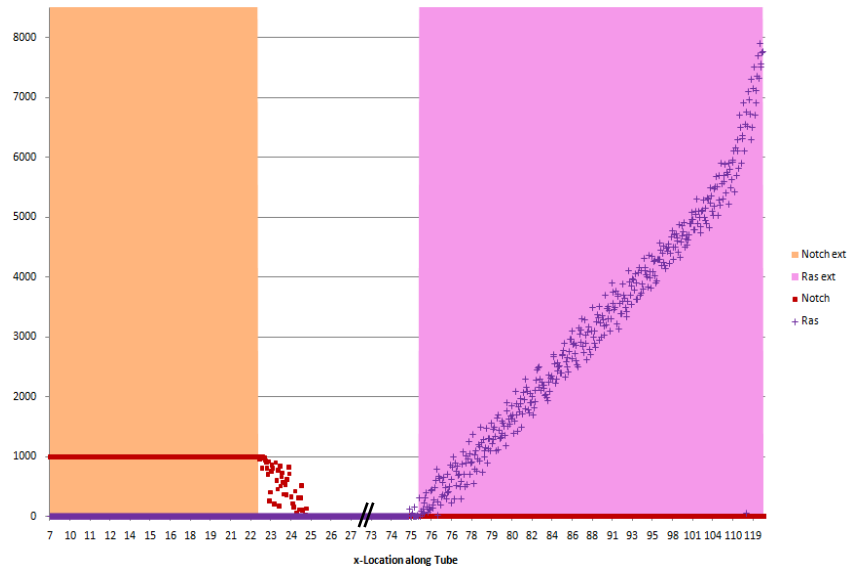
Fig. 12 Graph showing the Notch and Ras levels within the marked cells along with the status of external Delta and external Ras according to location in the germ line from the distal end up to the bend during the whole execution. The shaded area on the left indicates the region of the germ line where the Delta ligand is present (corresponding to mitotic region), the shaded area on the right signifies the same for the external Ras (corresponding to the region before the gonad bend). The squares represent the cell internal Notch levels, the crosses represent the internal Ras levels

Fig. 12 shows the dynamic behaviour of Notch and Ras within the marked cells according to their location between the distal end and the beginning of the loop in response to external signals. Similar to Fig. 10, we have excluded the range between 28 and 72 on the x-axis since the component levels do not change in this area. In the most distal part of the tube, the external Delta ligand of Notch signalling is present. Fig. 12 shows that, in response to this, all cells reach the maximal Notch level, which again decays in the absence of Delta. The figure further shows that some cells reach the lowest Notch level farther down the tube than others. Since, in each cell, the Notch level linearly decays over time at the same rate, this indicates a difference in speed of the marked cells. Fig. 12 also shows that in the presence of external Ras inducing signal, generally the Ras level within the cells constantly increases as they progress along the tube. There are a few cells before the area where the external Ras signal is present which nonetheless have an internal Ras level above 0. These are probably cells that were pushed back out of the Ras zone after having been in it for a short while. Similar to the speed of the cells relating to the Notch decay, Fig. 12 shows that there seems to be one cell at location 114 which still has a very low Ras level. Presumably, this cell was pushed much faster to this location than the other ones and has hence not had enough time to accumulate as much Ras. Apart from this single case, the Ras level does not

seem to fluctuate significantly, which indicates a mainly constant forward speed of the cells.

4 Discussion

In the present work, we have developed and calibrated a physical computational model of the *C. elegans* germ line. The model highlights a novel way of using molecular dynamics as a central engine of computational models simulating physical cell movement. The usage of the accurate physical features allows our model to be calibrated in a way that matches simulation and experimental time. The stress on physical features allows us to combine important developmental aspects such as cell division and growth in a realistic way. In addition, key molecular pathways, differentiation, and apoptosis are added, leading to a realistic model that can be used to an extensive analysis of our concept of the underlying system.

The usefulness of physical and Molecular Dynamics-like approaches to cell movement has been demonstrated in different settings (22; 24; 25; 27), mostly involving cell populations of tissues. In these models, especially the ones modelling more or less constant tissue-cell populations without cell divisions (24; 25), the physical movement caused by overlap of cells is only a by-product of an active movement along a chemical or nutritional gradient. In models including cell division (22; 27), this aspect of movement is more prominent but still limited due to nutrient dependence or contact inhibition. In our model, however, cells move purely due to physical compression by other cells arising from cell divisions and growth of cells. Our model visually represents this compression by overlap of the circles. To our knowledge, the present model is the first to simulate cell movement purely based on these physical aspects without any active migration. The lack of active movement in our model is in accordance with the experimental observations in the biological system (28; 29).

While still a simplified representation of the germ line, our model produces cell movement that looks very natural, and we were able to calibrate the model in accordance to different experimental observations found in the literature (15; 19; 28) as well as from our own experiments. We have used the cell movement rate derived from our own observations and (28; 29) to incorporate a measure of real time in our model. The comparison allowed us to identify the approximate number of time steps in our model that represents an hour in real time. Based on this value, the division rate from our model is very much in accordance with the one observed in the literature (28). The same is true for the death rates that we observed in the model and experimentally. Only the fertilisation rate differed slightly from the value in the literature (15). Furthermore, the value might change after including the rachis in a revised version of our model, which will change the cell movement close to the end of the germ line. In addition to calibrating, our model allows us to observe properties of single marked cells like density factor, size and kinetics

at any timepoint. These aspects can be used in the future to test or evolve new hypotheses like density dependent apoptosis or time-dependent developmental progression of individual cells. Furthermore, these parameters allow feeding the model by results from wet lab experimentation and vice versa. Conclusively, our physical MD modelling approach can be very useful in this setting and extensions to the present model promises to advance our understanding of fundamental biological processes.

5 Future Prospects

We will try to overcome certain limitations of our current simplified model. Including the rachis into our model is very important as this might improve the values of the death and fertilisation rates and will render the model as a whole visually more realistic. Further, extending the abstract "Notch" and "Ras" signalling pathways by their individual regulatory components could help to gain a more detailed understanding of the biological system.

The successful calibration of our model renders it amenable to testing hypotheses about the germ line system and about specific aspects of development. Our major goal will be to test different possible mechanisms of apoptosis. It is known that about 50% of all potential oocytes die; one likely explanation is the need for nurse cells that synthesise enough cytoplasm for the rapidly growing oocytes (15; 19). So far it is unclear how the decision is taken when and which of the cells should die. A probable explanation is that there is a balance between the cytoplasm being produced and the number of cells allowed to progress (19). Still, apoptosis could be random or clearly determined by aspects like Ras activity level, developmental timing or cell size. Another very interesting aspect of the germ line is the question of symmetric versus asymmetric division of stem cells. It has not been fully resolved whether the post-larval germinal stem cells divide symmetrically or asymmetrically, i.e. if both daughter cells retain stem cell properties and can divide further, or if only one of the daughter cells remains in the mitotic zone whereas the sister progresses toward maturation into a gamete, respectively. The prevailing model assumes that the division happens symmetrically (33). Still, some of the cells might remain in the mitotic zone if they are not pushed by other dividing cells (28). We will focus our future modelling work on these two and other sparsely understood aspects of the *C. elegans* germ line to gain further understanding and generate input for wet lab experiments that can validate the model's predictions.

1.   Brenner S. The genetics of Caenorhabditis elegans. Genetics. 1974 May ;77(1):71-94.

2.   Hillier LW, Coulson A, Murray JI, Bao Z, Sulston JE, Waterston RH. Genomics in C. elegans: so many genes, such a little worm. Genome research. 2005 Dec ;15(12):1651-60.

3.   Potts MB, Cameron S. Cell lineage and cell death: Caenorhabditis elegans and cancer research. Nature Reviews Cancer. 2010 Dec ;11(January):50-58.

4.   Joshi PM, Riddle MR, Djabrayan NJV, Rothman JH. Caenorhabditis elegans as a model for stem cell biology. Developmental dynamics : an official publication of the American Association of Anatomists. 2010 May ;239(5):1539-54.

5.   Riddle DL, Blumenthal T, Meyer BJ, Priess JR. C. elegans II. CSHL Press; 1997.

6.   Corsi AK. A biochemist's guide to Caenorhabditis elegans. Analytical biochemistry. 2006 Dec ;359(1):1-17.

7.   Sulston J. Post-embryonic cell lineages of the nematode, Caenorhabditis elegans. Developmental Biology. 1977 Mar ;56(1):110-156.

8.   Kipreos ET. C. elegans cell cycles: invariance and stem cell divisions. Nature reviews. Molecular cell biology. 2005 Oct ;6(10):766-76.

9.   Hubbard EJA, Greenstein D. Introduction to the germ line. WormBook : the online review of C. elegans biology. 2005 Jan ;1-4.

10.   Kimble J, Crittenden SL. Germline proliferation and its control. WormBook : the online review of C. elegans biology. 2005 Jan ;1-14.

11.   Gartner A, Boag PR, Blackwell TK. Germline survival and apoptosis. WormBook : the online review of C. elegans biology. 2008 Jan ;1-20.

12.   Korta DZ, Hubbard EJA. Soma-germline interactions that influence germline proliferation in Caenorhabditis elegans. Developmental dynamics : an official publication of the American Association of Anatomists. 2010 May ;239(5):1449-59.

13.   Hanahan D, Weinberg RA. Hallmarks of Cancer: The Next Generation. Cell. 2011 Mar ;144(5):646-674.

14.   Krantic S, Mechawar N, Reix S, Quirion R. Molecular basis of programmed cell death involved in neurodegeneration. Trends in neurosciences. 2005 Dec ;28(12):670-6.

15.   Hirsh D, Oppenheim D, Klass M. Development of the reproductive system of Caenorhabditis elegans. Developmental biology. 1976 Mar ;49(1):200-19.

16.   Hansen D, Hubbard EJA, Schedl T. Multi-pathway control of the proliferation versus meiotic development decision in the Caenorhabditis elegans germline. Developmental biology. 2004 Apr ;268(2):342-57.

17.   Kimble J, White J. On the control of germ cell development in Caenorhabditis elegans• 1. Developmental Biology. 1981 ;81(2):208–219.

18.   Waters K a, Reinke V. Extrinsic and intrinsic control of germ cell proliferation in Caenorhabditis elegans. Molecular reproduction and development. 2011 Jan ;160151-160.

19.   Gumienny TL, Lambie E, Hartwieg E, Horvitz HR, Hengartner MO. Genetic control of programmed cell death in the Caenorhabditis elegans hermaphrodite germline. Development (Cambridge, England). 1999 Feb ;126(5):1011-22.

20.   Church DL, Guan KL, Lambie EJ. Three genes of the MAP kinase cascade, mek-2, mpk-1/sur-1 and let-60 ras, are required for meiotic cell cycle progression in Caenorhabditis elegans. Development (Cambridge, England). 1995 Aug ;121(8):2525-35.

21.   Alder BJ, Wainwright TE. Studies in Molecular Dynamics. I. General Method. The Journal of Chemical Physics. 1959 Aug ;31(2):459.

22.   Drasdo D, Kree R, McCaskill J. Monte Carlo approach to tissue-cell populations. Physical review E. 1995 ;52(6):6635–6657.

23.   Beyer T, Meyer-Hermann M. Modeling emergent tissue organization involving high-speed migrating cells in a flow equilibrium. Physical Review E. 2007 Aug ;76(2):27.

24.   Beyer T, Meyer-Hermann M. Multiscale modeling of cell mechanics and tissue organization. IEEE engineering in medicine and biology magazine : the quarterly magazine of the Engineering in Medicine & Biology Society. 2009 ;28(2):38-45.

25.   Palsson E. A three-dimensional model of cell movement in multicellular systems. Future Generation Computer Systems. 2001 May ;17(7):835-852.

26.   Palsson E, Othmer HG. A model for individual and collective cell movement in Dictyostelium discoideum. Proceedings of the National Academy of Sciences of the United States of America. 2000 Sep ;97(19):10448-53.

27.   Schaller G, Meyer-Hermann M. Multicellular tumor spheroid in an off-lattice Voronoi-Delaunay cell model. Physical Review E. 2005 May ;71(5):1-16.

28.   Crittenden SL, Leonhard KA, Byrd DT, Kimble J. Cellular analyses of the mitotic region in the Caenorhabditis elegans adult germ line. Molecular biology of the cell. 2006 Jul ;17(7):3051-61.

29.   Maciejowski J, Ugel N, Mishra B, Isopi M, Hubbard EJA. Quantitative analysis of germline mitosis in adult C. elegans. Developmental biology. 2006 Apr ;292(1):142-51.

24

30.   Swope WC. A computer simulation method for the calculation of equilibrium constants for the formation of physical clusters of molecules: Application to small water clusters. The Journal of Chemical Physics. 1982 ;76(1):637.

31.   Microsoft. Visual F# - Documentation [Internet]. 2011 ;[cited 2011 Mar 9] Available from: http://msdn.microsoft.com/library/dd233154(VS.100).aspx

32.   Accompanying movie [Internet]. 2011 ;[cited 2011 Mar 27] Available from: http://www.cs.le.ac.uk/people/npiterman/publications/2011/BEPHHF/index.html

33.   Cinquin O, Crittenden SL, Morgan DE, Kimble J. Progression from a stem cell-like state to early differentiation in the C. elegans germ line. Proceedings of the National Academy of Sciences of the United States of America. 2010 Feb ;107(5):2048-53.